
Assessment of Malignancy in Pulmonary Lesions: FDG Dual-Head Coincidence Gamma Camera Imaging in Association with Serum Tumor Marker Measurement

Valérie Bousson, Jean-Luc Moretti, Pierre Weinmann, Nour Safi, Feyzi Tamgac, Corinne Groiselle, Virginie de Beco, Younes Hillali, Dominique Valeyre, and Jean-Luc Breaux

Departments of Nuclear Medicine, Oncology, and Pulmonary Medicine, CHU, Paris, Bobigny; and Department of Statistics, CHU, Dauphine, France

The purpose of the study was to evaluate the performance of dual-head coincidence gamma camera imaging using FDG in association with serum marker assays in identifying lung carcinoma in patients with abnormal findings on chest radiography. **Methods:** A prospective evaluation of FDG imaging with coincidence detection emission tomography (CDET) using a dual-head gamma camera combined with the assessment of 3 sensitive serum markers of lung cancer (carcinoembryonic antigen, neuron specific enolase, and CYFRA 21-1) was performed on the same day on 58 consecutive patients with known or suspected lung malignancy. **Results:** Fifty-three patients were proven to have lung cancer, and 5 patients had benign lung disease. Coincidence imaging showed significantly increased FDG uptake in 49 of 53 patients with proven malignancy (sensitivity, 92.5%) and in 3 patients with benign disease. FDG imaging had negative findings in 4 patients with proven malignancy and 2 patients with benign disease. Serum tumor marker levels were elevated in 42 of 53 cancer patients (sensitivity, 79.2%) and normal in 11 patients with proven malignancy. Nine patients with proven malignancy had positive findings on FDG images and negative marker assays. Two patients with proven malignancy had negative findings on FDG images and positive marker assays. The positive predictive value for lung cancer was 94.2% for FDG alone and 97.6% for FDG in association with serum markers. **Conclusion:** In this study, FDG CDET imaging was a powerful tool for evaluating patients with lung lesions suggestive of malignancy. Although the determination of serum marker levels was less accurate than FDG imaging, positive FDG results found in association with positive markers significantly increased the likelihood of lung malignancy.

Key Words: FDG; dual-detector coincidence imaging; pulmonary lesions; serum markers

J Nucl Med 2000; 41:1801-1807

The incidence of lung cancer is increasing in all countries, and nearly 200,000 new cases are diagnosed every year in the United States (1). Five-year survival for non-small cell lung cancer is 42%, 22%, 5%, and 3% for stages I, II, III, and IV, respectively (2).

FDG PET is currently performed to assess the increased glucose metabolism in tumor cells (3). Until recently, positron imaging with FDG in patients with known or suspected lung cancer was performed with dedicated PET scanners, and numerous studies have shown the value of FDG PET in characterizing lung nodules (4,5), in evaluating lung cancer (6), in staging non-small cell lung cancer (7), and in determining the prognosis for overall survival (8). Given the high cost and limited availability of FDG PET (9), 2 alternative methods have been developed to detect the 511-keV photons of positron emitters. The first was to use 511-keV collimators in a way similar to usual SPECT (10). This approach showed poor sensitivity and poor spatial resolution (11). A second approach, more encouraging, uses a conventional dual-head gamma camera fitted with coincidence electronic hardware to allow coincidence detection emission tomography (CDET) (12) or gamma camera PET. In addition to its relatively lower cost, this approach has the advantage of being able to detect a wide range of photon energies, allowing its use in routine nuclear medicine practice.

A main limitation of CDET is the counting rate of the gamma camera (no more than 1.5 million cps in our system) (13,14), but substantial scattering from false coincidence events (spatial mispositioning of events) and lack of attenuation correction are also limiting factors. However, software such as iterative image reconstruction algorithms has been developed to improve image quality (15,16). Compared with filtered backprojection, these algorithms improve the image-to-noise ratio and better reduce artifacts around hot spots (17). In this study, our goal was to assess the overall diagnostic performance of 3 serum tumor markers in conjunction with FDG CDET for the detection of lung cancer.

Assessment of tumor marker levels is widely used to

Received Sep. 8, 1999; revision accepted Mar. 2, 2000.

For correspondence or reprints contact: Jean-Luc Moretti, MD, PhD, Department of Nuclear Medicine, Avicenne Hospital, 125 rue de Stalingrad, Bobigny F 93009, France.

screen for early cancer, to assess the efficiency of cancer therapy, and to indicate the recurrence and progression of disease. Among the variety of tumor markers used clinically for lung cancer, the most accurate and frequently chosen are carcinoembryonic antigen (CEA) (18), CYFRA 21-1 (19), and neuron-specific enolase (NSE) (20,21). Measurement of more than 1 tumor marker is advisable for improving diagnostic accuracy (22). CEA plus CYFRA 21-1, CYFRA 21-1 plus cell carcinoma antigen, and CYFRA 21-1 plus NSE are helpful combinations for diagnosing adenocarcinoma, squamous cell carcinoma, and small cell carcinoma, respectively (23).

MATERIALS AND METHODS

From October 1997 to December 1998, we performed a single-institution prospective evaluation of the overall diagnostic performance of FDG imaging with CDET in association with the assessment of 3 serum markers of lung cancer.

Patient Population

Men and women (>18 y old) admitted to the Department of Pulmonary Disease of our hospital were eligible to enter the study if their chest radiograph or CT scan showed an abnormality known or strongly suspected to represent lung cancer and if they were not pregnant, had no history of diabetes, could tolerate coincidence imaging, and could provide written informed consent for the study. Surgery or tissue sampling planned to occur within 1 mo of scanning were highly recommended but not mandatory to enter the study.

Sixty-nine consecutive patients meeting the criteria were enrolled. Table 1 summarizes the patient data. For 53 patients, FDG imaging and tumor marker evaluation were part of an initial evaluation after abnormalities had been found on chest radiography or CT. For 16 patients, the evaluation was the second for a previously known case of chest or colorectal cancer with suspected lung metastases. A histologic examination was performed for 58 of 69 patients (46 men, 12 women; age range, 23–81 y; mean age \pm SD, 56 ± 11.3 y). Lung biopsy could not be performed for the remaining 11 patients, and these patients were not included.

TABLE 1
Histologic Results for Enrolled Patients

Characteristic	No. of patients (of 58 total)
Proven benign lung disease	5
Tuberculosis	2
Inflammatory pseudotumor	2
Inflammatory granuloma	1
Proven malignant lung disease	53
Non-small cell lung carcinoma	
Adenocarcinoma	26
Squamous cell carcinoma	10
Large cell carcinoma	6
Mixed carcinoma	1
Bronchioloalveolar carcinoma	2
Small cell lung carcinoma	3
Mesothelioma	1
Secondary lung cancer	4

Imaging Protocols

Coincidence-mode imaging was performed on a dual-detector gamma camera modified to allow detection of 511-keV gamma emission from positrons (Vertex; ADAC Laboratories, Milpitas, CA). A 1.6-cm-thick sodium iodide crystal detector was used. The purpose was to improve detection efficiency for the 511-keV photons from 1.7% to 4.4% (13). The coincidence mode of acquisition used all photopeak-to-photopeak events as well as the photopeak-to-Compton scatter events. Compton-to-Compton events were not used. The energy windows were set at 511 keV with a 30% window width percentage for the FDG photopeak and at 310 keV with the same window width for the Compton events.

The coincidence counting rate for the entire reconstructed field of view was 30×10^3 coincidence events per second. The sensitivity of our CDET was 2.7 kcps/kBq/mL, with a maximum counting rate of 13,800 events per second. The detector time resolution was 6 ns, and a 15-ns timing window was used to acquire coincidence events. FDG was produced in the Cyclotron of the University of Brussels (Erasmus Hospital) and delivered to our department twice a week.

All patients fasted for at least 4 h before the administration of FDG. The serum glucose level was measured for all patients. Sixty to 90 min before scanning, the patients received an intravenous injection of 100–200 MBq FDG while lying in a silent room. During the lag between injection and scanning, the patients were asked to remain still to avoid excessive FDG uptake in striated muscles. The acquisition was obtained after bladder voiding. Thirty-two steps were performed through a rotation of 180° per detector, with 40 s per step, for a total acquisition time of 23 min per bed position.

Two bed positions were used, 1 for the chest and 1 for the abdomen, with a scan overlap of 50% and a 57-cm resulting field of view. Data were acquired in 3-dimensional mode with decay correction during the acquisition. The total counts in the projection data ranged from 20 to 30 million counts per bed position.

After rebinning, data were processed with an ordered-subset expectation maximization iterative algorithm. Parameters used to perform the iterative reconstruction included an ordered subset of 8 with a Wiener prefilter and a noise factor of 0.7 with 2 iterations. Images were reconstructed into a $128 \times 128 \times 16$ volume of 4-mm cubic voxels. Data were not corrected for attenuation.

Image Analysis

FDG images were interpreted by 3 independent observers on an interactive computer system (Sun Sparc 20; ADAC Laboratories) with use of both a linear gray scale and a linear thermal color scale with 10% background subtraction. The 3 observers knew the age and sex of the patient and the location of the suspected cancer but not the serum marker level. An initial visual evaluation (transverse, coronal, and sagittal slices of 4-mm width) detected nonpathologic focal areas of FDG uptake. They were graded with the consensus of the 3 observers on a 3-point scale: 2 = abnormal, 1 = equivocal uptake, and 0 = normal. In cases of equivocal lesion uptake, grading was done with the help of a semiquantitative evaluation of the FDG images. Lesion uptake was expressed as lesion-to-background mean count ratio (L/B), using axial and coronal slices. The highest L/B was selected. A circular region of interest was drawn 1 pixel inside the borders of the tumor to limit the partial-volume effect. Because our images were analyzed without attenuation correction, a symmetric circular area of the same size was drawn in the contralateral lung as background. This area was positioned optimally in a site, taking into account its depth, to provide a measure independent of the location of the lesion. An adjacent lung area was chosen when the

contralateral lung area was abnormal. An adjacent mediastinal area was chosen for mediastinal tumors.

FDG scintigraphy was considered positive for malignancy when at least 1 hyperactive lesion had a grade of 2 or a grade of 1 with a semiquantitative L/B superior to 1.4. A cutoff of 1.4 was chosen because this value was previously defined to be the minimum at which lesion contrast can be detected (24).

Serum Tumor Marker Evaluation

Blood samples from all 69 patients were obtained before FDG injection, and the serum was stored at -20°C . Levels of CYFRA 21-1 and NSE were measured using Kryptor and Trace commercial kits from CIS Bio International (Gif-Sur-Yvette, France), and levels of CEA were measured using Cobas Core CEA EIAII (Roche Diagnostics, Meylan, France). The respective thresholds were 3.5 ng/mL, 10 ng/mL, and 4 ng/mL. The tumor marker evaluation was considered positive for malignancy when the serum level of at least 1 tumor marker was elevated.

Statistical Analysis

The statistical significance of differences between the performance of the 2 methods was assessed using a proportion test that considered only pathologically proven cases of lung carcinoma. The level of significance was set at $P < 0.05$. Positive predictive values were assessed using FDG imaging results alone and in association with serum marker levels.

RESULTS

Histologic Findings

Histologic findings (Table 1) were positive for malignancy in 53 of 58 eligible patients from whom biopsy samples could be obtained. The malignancies that were diagnosed included adeno-

carcinoma ($n = 26$), squamous cell carcinoma ($n = 10$), large cell carcinoma ($n = 6$), mixed cell carcinoma ($n = 1$), bronchioloalveolar carcinoma ($n = 2$), small cell carcinoma ($n = 3$), colorectal metastases ($n = 4$), and mesothelioma ($n = 1$). In 5 patients, benign lesions were diagnosed pathologically, including tuberculosis ($n = 2$), pulmonary inflammatory pseudotumors ($n = 2$), and inflammatory granuloma ($n = 1$).

FDG Images

FDG images revealed focal areas of significantly increased FDG uptake (grade 2) in the region of the radiographic nodules in 52 patients: 49 patients with proven malignancy and 3 patients with proven benign disease (1 case each of inflammatory granuloma, inflammatory pseudotumor [Fig. 1], and tuberculosis [Fig. 2]). FDG images were negative for FDG uptake in 6 patients (grade 0 or 1): 2 patients with proven benign disease (1 case each of tuberculosis and pseudotumor) and 4 patients with lung cancer (1 case of equivocal adenocarcinoma [Fig. 3], 2 of bronchioloalveolar carcinoma, and 1 of multiple 5-mm-diameter metastases from colorectal carcinoma). The results are summarized in Table 2.

FDG imaging was more sensitive ($P = 0.0256$) at detecting lung cancer than were the 3 tumor markers. When FDG imaging and the tumor marker assays were considered together, the positive predictive value was 97.6%.

Serum Tumor Markers

The serum marker evaluation was positive for malignancy in 43 patients and negative in 15 patients. Among the patients with positive findings, 42 had proven malignancy

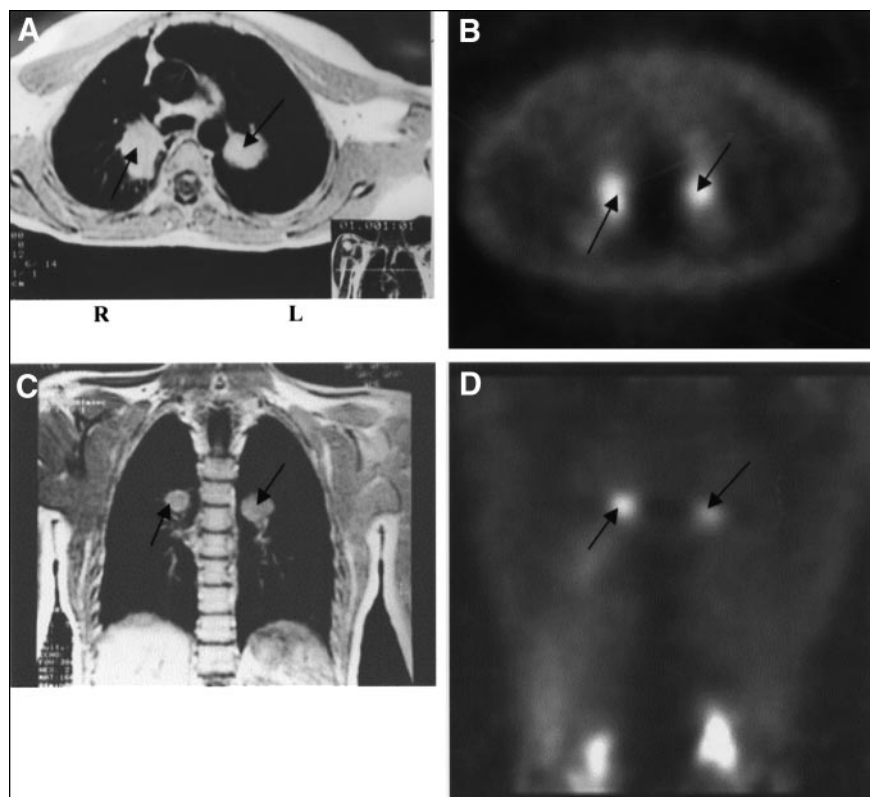


FIGURE 1. False-positive FDG finding in 23-y-old woman with inflammatory pseudotumors. Transverse (A) and coronal (B) T1-weighted MR images show 2 well-defined nodular masses (arrows), with slightly hyperintense signal intensity compared with muscles. Transverse (C) and coronal (D) FDG images obtained at same level as (A) and (B) show 2 foci of abnormal FDG uptake (arrows) (right L/B, 2.9; left L/B, 3.9).

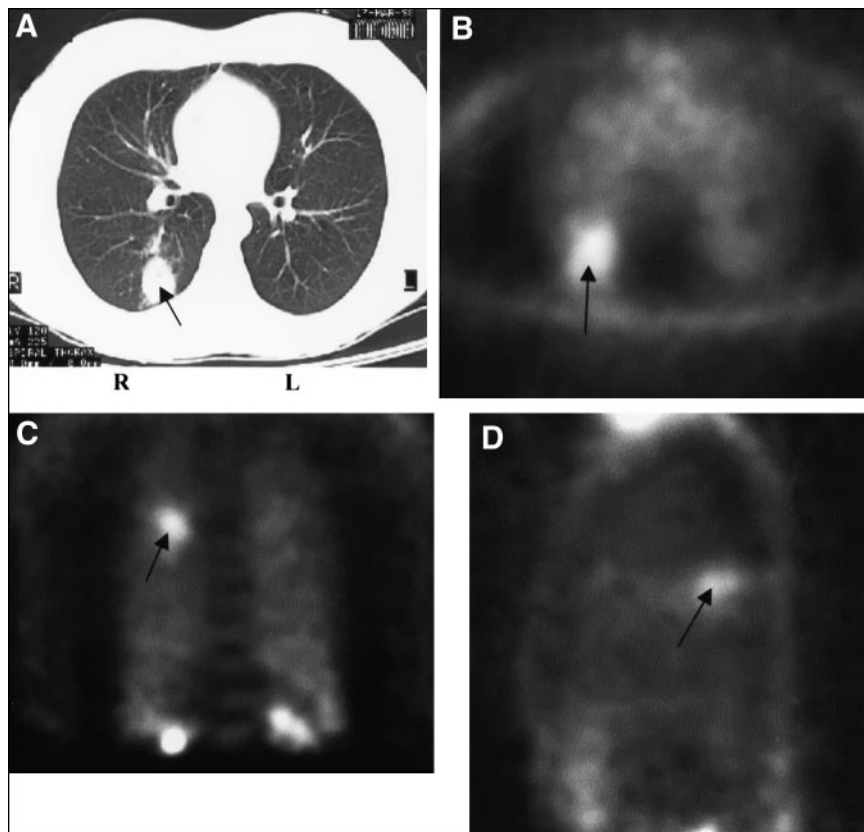


FIGURE 2. False-positive FDG finding in 39-y-old woman with pulmonary tuberculosis. (A) Unenhanced chest CT image shows excavated posterior mass (arrow) in upper right lobe. (B) Transverse FDG image obtained at same level as (A) shows focal FDG uptake (arrow) (L/B, 2.4). Coronal (C) and sagittal (D) FDG images show hot lesion in upper right lobe (arrow).

and 1 had proven benign disease (tuberculosis). Eleven patients with proven malignancy had negative findings on serum marker evaluation. The sensitivity of tumor marker evaluation was 79.2%. The results are summarized in Table 2. Discordances between FDG imaging and serum tumor marker evaluations are shown in Table 3.

DISCUSSION

PET can image metabolic differences between normal and malignant cells. Malignant cells exhibit increased glucose metabolism (3) and glucose transporter Glut1 activity (25). Subsequent studies have documented the accuracy of FDG

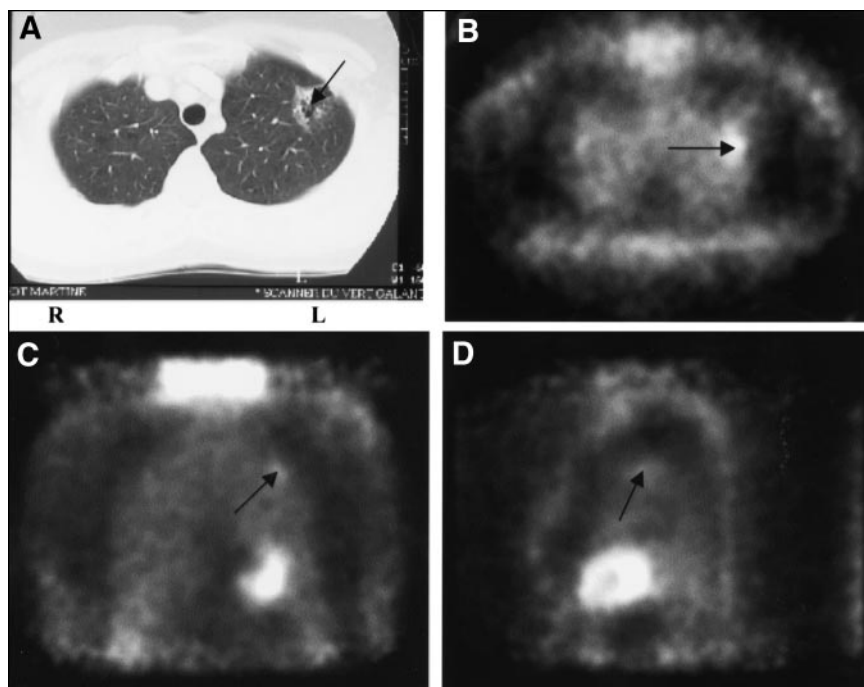


FIGURE 3. Equivocal FDG finding in 48-y-old woman with false-negative case of lung adenocarcinoma. (A) Unenhanced chest CT image shows excavated 3-cm-diameter lesion (arrow) in left upper lobe. (B) FDG transverse image obtained at same level as (A) shows abnormal FDG uptake considered equivocal by visual analysis and on cutoff line for malignancy (arrow) (L/B, 1.4). Coronal (C) and sagittal (D) FDG images show faint hyperactive lesion (arrow) in upper left lobe (L/B, 1.3) under cutoff line for malignancy.

TABLE 2
Results of FDG Imaging and Tumor Marker Evaluation

Tumor marker finding	FDG finding			
	Positive		Negative	
	Malignant	Benign	Malignant	Benign
Positive	40	1*	2	2†
Negative	9	2‡	2	0

*Tuberculosis.

†Tuberculosis, pseudotumor.

‡Inflammatory granuloma.

PET in detecting and staging various malignancies (especially lung malignancies) (4–8). Recent studies have compared PET with CDET for lung cancer imaging and concluded that CDET cannot be considered completely equivalent to full-ring PET scanners but can provide adequate diagnostic information. FDG CDET showed a relatively high sensitivity in detecting lung nodules (93%) and a moderate sensitivity (65%) for mediastinal lesions (14,26). In our study, the sensitivity for lung cancer detection was 92.5%, which is similar to the 93% sensitivity found by Shreve et al. (14), who used the same CDET camera (14).

Delbeke et al. (26) reported a lower sensitivity (73%) in detecting malignancy, but the interval between injection and imaging was shorter than ours (mean, 73 min) and the NaI(Tl) crystal was thinner (0.95 cm versus 1.6 cm thick). Their study yielded a relative sensitivity of 85% for CDET, compared with PET, for lesions more than 1.2 cm in size (26).

Two other studies on FDG CDET of pulmonary lesions were recently performed on 23 (27) and 96 (28) patients. The first study concluded that the sensitivity of CDET, compared with PET, was 0.96. The second study showed that FDG CDET was 97% sensitive and 80% specific in identifying proven malignant lesions (28). Our results are similar to those of these 2 studies.

In our study, 3 cases of false-positive foci were found. These solitary pulmonary nodules were read as malignant on chest CT scans and as hypermetabolic on FDG images but proved to be a tuberculous lesion, an inflammatory pseudotumor, and a granuloma. The presence of active inflammatory disease is a common cause of false-positive findings. Increased FDG uptake has been reported in inflammatory or infectious processes such as aspergillosis, tuberculosis, histiocytosis, sarcoidosis, and some benign tumors (29,30). Although the metabolic rate in an inflammatory process is usually substantially less than in neoplastic tissue, some overlap exists between FDG uptake by malignant lesions and severe infectious foci such as pneumonia (31). In our semiquantitative evaluation, we chose a 1.4 threshold for the L/B on the basis of a previous investigation (32). In our study, the L/Bs of the 3 falsely positive benign lesions were significantly higher than our chosen threshold, but this finding could be explained by the marked inflammatory reaction that histologic examination disclosed.

In 4 patients with malignant lesions, FDG imaging findings were negative. Two patients had large bronchioloalveolar lung carcinomas. Negative results with FDG imaging for that subtype of adenocarcinoma have already been reported (33,34) and can be caused by a low metabolic

TABLE 3
Analysis of False-Negative Results for FDG Imaging and Tumor Marker Evaluation

False-negative finding	Histologic finding	L/B	Markers			Size of main lesion (cm)	Previous treatment
			ACE	CYFRA 21-1	NSE		
FDG positive, markers negative	Adenocarcinoma	1.8	2.5	5.8	0.2	2 × 2 (CT)	ChT and chest Rt ending 1 mo earlier
	Adenocarcinoma	2.7	1.3	6.5	3.3	3.6 × 3 (CT)	None
	Adenocarcinoma	1.7	2.4	8.6	1.0	3 × 3 (CT)	None
	Adenocarcinoma	4.8	3.9	7.4	0.5	2 × 2 (CT)	None
	Adenocarcinoma	1.6	3.7	4.4	0.7	5 × 4.5	None
	Large cell carcinoma	1.6	2.3	6.9	2.1	3	None
	Squamous cell carcinoma	1.6	2.3	5.1	0.7	2 × 2 (CT)	ChT and chest Rt ending 7 mo earlier
	Lung metastases	1.8	2.4	8.4	1.2	4	ChT and chest Rt ending 1 mo earlier
FDG negative, markers positive	Mixed carcinoma	2.8	2.9	5.7	1.0	3 × 2.5	None
	Adenocarcinoma	1.4	4.6	4.2	0.6	2 × 2.5	None
FDG negative, markers negative	Bronchioloalveolar carcinoma	1	4.3	5.8	0.4	6	None
	Lung metastases	1	2.5	5.6	0.4	1 × 1 (CT)	Pelvic surgery and ChT ending 1 y earlier
	Bronchioloalveolar carcinoma	1	3.7	5.0	0.4	4 × 3	ChT and chest Rt ending 2 mo earlier

ChT = chemotherapy; Rt = radiotherapy.

demand for glucose by slow-growing bronchioloalveolar carcinoma and the presence of relatively few metabolically active malignant cells (34). In the 2 other patients (1 with adenocarcinoma and 1 with multiple colorectal lung metastases smaller than 1 cm in diameter), false-negative findings could have been caused by the small size of the lesions.

Scintigraphic detection of malignant lesions proceeds from uptake of FDG and the ratio with surrounding tissues. Because of soft-tissue attenuation and the low FDG background activity of normal lung, detection of malignant lesions is easier in the lungs than in other organs.

With FDG imaging, L/B may be useful for differentiating between benign and malignant lesions. L/Bs with a dual-head gamma camera are not as high as with dedicated PET systems, for which ratios range from 3:1 to 10:1 (35). The lower ratios observed with CDET imaging are probably caused by current limitations.

Nine patients with proven malignancy had no elevation of any tumor marker but had positive FDG imaging findings (Table 3). The lesions included 5 cases of adenocarcinoma, 1 of large cell carcinoma, 1 of squamous cell carcinoma, 1 of mixed carcinoma, and 1 of colorectal lung metastases. Six patients had received no treatment before FDG imaging and assessment of the 3 marker levels. Three patients received recurrent treatment before FDG imaging and assessment of the 3 marker levels. Two patients had elevated levels of tumor markers but no significant FDG uptake (Table 3). They presented with bronchioloalveolar carcinoma and grade I adenocarcinoma. In these 2 patients, the findings of tumor marker evaluation had been considered positive according to the defined criteria, but the positivity was caused by a slightly elevated CEA level only (4.1 and 5.7, with a cutoff value of 4 ng/mL).

Generally, more than 90% of healthy individuals have a CEA serum concentration less than 2.5 ng/mL. Elevated CEA levels may occur in smokers or patients with chronic obstructive pulmonary disease, and CEA levels are related to age (35–38). Elevated levels usually remain less than the threshold value. Fukuda et al. (36) reported a CEA level elevated by approximately 1.0 ng/mL in male heavy smokers (3.11 ng/mL instead of 2.14 ng/mL, which remains less than the threshold value) for a series of 1341 subjects. However, 32 male heavy smokers (smoking index > 200) had a serum CEA value greater than the threshold value used by the investigators. At least 3 of our 5 patients (exact tobacco consumption was not known for the 2 other patients) were current heavy smokers.

CDET is limited in tumors smaller than 2 cm in diameter, because partial-volume effects cause the uptake intensity to be dependent on tumor size. This limitation is the reason that we drew a region of interest within the borders of the lesions.

Thresholds used for both FDG diagnosis and tumor marker levels were chosen to avoid subjective reading. But none of these thresholds may be interpreted as an absolute test for malignant disease.

The studied population was heterogeneous, including

patients with various stages of lung cancer, variable treatments, and different types of histology. This heterogeneity reflects clinical practice and will require a focused prospective investigation for each type of lesion.

Our study did not allow an assessment of the specificity of both techniques, because the study included only a limited number of patients with benign condition.

Our 91% prevalence of lung cancer led to an artificially high positive predictive value. However, during the course of this study 9 patients did not undergo surgery because of a high risk of complications. All these patients are currently free of cancer at 1 y. These data reinforce our results and show the clinical impact of FDG CDET in patient management.

CONCLUSION

Medical practice today tends to be more closely monitored and assessed for cost-effectiveness. Oncologists are accustomed to testing several serum markers for determining the diagnosis, stage, and prognosis of tumors and for monitoring patients with lung cancer. But assessing the real benefit of serum markers in patient management is difficult. FDG PET has been proven accurate and cost-effective for staging non-small cell lung cancer (39).

Accuracy and cost-effectiveness remain to be confirmed for FDG imaging with a modified dual-head gamma camera. Our preliminary results indicate that FDG imaging with such a camera is more sensitive at detecting malignancy in patients with suspected lung cancer than is measurement of the 3 most sensitive serum markers for lung cancer.

Our results advocate further prospective evaluation of the value of FDG imaging with a modified dual-head gamma camera (CDET) in the management of lung cancer and the use of such imaging in association with serum marker determination.

ACKNOWLEDGMENTS

The authors thank Dr. Georges Baillet for his helpful assistance. This study was sponsored by grants allocated to the University Hospital of Bobigny from ARC, Clinical Research of Assistance Publique de Paris (PHRC 95), Department of Seine Saint-Denis, and Banque de la Vie Recherche Cancer, France. This study was presented in part at the annual meeting of the Society of Nuclear Medicine, Los Angeles, CA, June 1999.

REFERENCES

1. Beckett WS. Epidemiology and etiology of lung cancer. *Clin Chest Med.* 1993;14:1–15.
2. Fry WA, Menck HR, Winchester DP. The national cancer data base report on lung cancer. *Cancer.* 1996;77:1947–1955.
3. Nolop KB, Rhodes CG, Brudin LH, et al. Glucose utilization in vivo by human pulmonary neoplasm. *Cancer.* 1987;60:2682–2689.
4. Lowe VJ, Fletcher JW, Gobar L, et al. Prospective investigation of positron emission tomography in lung nodules. *J Clin Oncol.* 1998;16:1075–1084.
5. Gupta NC, Maloof J, Gunel E. Probability of malignancy in solitary pulmonary nodules using fluorine-18-FDG and PET. *J Nucl Med.* 1996;37:943–948.

6. Lewis P, Griffin S, Marsden P, et al. Whole-body ¹⁸F-fluorodeoxyglucose positron emission tomography in preoperative evaluation of lung cancer. *Lancet*. 1994;344:1265–1266.
7. Bury T, Dowlati A, Paulus P, et al. Whole-body ¹⁸FDG positron emission tomography in the staging of non-small cell lung cancer. *Eur Respir J*. 1997;10:2529–2534.
8. Ahuja V, Coleman RE, Herndon J, Patz EF. The prognostic significance of fluorodeoxyglucose positron emission tomography imaging for patients with nonsmall cell lung carcinoma. *Cancer*. 1998;83:918–924.
9. Conti PS, Keppeler JS, Halls JM. Positron emission tomography: a financial and operational analysis. *AJR*. 1994;162:1279–1286.
10. Van Lingen A, Huijgens PC, Visser FC, et al. Performance characteristics of a 511-KeV collimator for imaging positron emission with a standard gamma camera. *Eur J Nucl Med*. 1992;19:315–321.
11. MacFarlane DJ, Cotton L, Ackermann RJ, et al. Triple-head SPECT with 2-[fluorine-18]fluoro-2-deoxyglucose (FDG): initial evaluation in oncology and comparison with FDG PET. *Radiology*. 1995;194:425–429.
12. Drane WE, Abott FD, Nicloe MW, Mastin ST, Kuperus JH. Technology for FDG-SPECT with a relatively inexpensive gamma-camera (work in progress). *Radiology*. 1994;191:461–465.
13. Patton A, Turkington G. Coincidence imaging with a dual-head scintillation camera. *J Nucl Med*. 1999;40:432–441.
14. Shreve PD, Steventon RS, Deters EC, Kison PV, Gross MD, Wahl RL. Oncologic diagnosis with 2-[fluorine-18]fluoro-2-deoxy-D-glucose imaging: dual-head coincidence gamma camera versus positron emission tomographic scanner. *Radiology*. 1998;207:431–437.
15. Hutton BF, Hudson HM, Beekman FJ. A clinical perspective of accelerated statistical reconstruction. *Eur J Nucl Med*. 1997;24:797–808.
16. Phelps ME, Cherry SR. The changing design of positron imaging systems. *Clin Positron Imaging*. 1998;1:31–45.
17. Zasadny KR, Kison PV, Quint LE, Wahl RL. Untreated lung cancer: quantification of systematic distortion of tumor size and shape on non-attenuation-corrected 2-[fluorine-18]fluoro-2-deoxy-D-glucose PET scans. *Radiology*. 1996;201:873–876.
18. Gold P, Freedman SO. Specific carcinoembryonic antigens of the human digestive system. *J Exp Med*. 1965;122:467–481.
19. Broers JL, Ramaekers FCS, Rot MK, et al. Cytokeratins in different type of human lung cancer as monitored by chain-specific monoclonal antibodies. *Cancer Res*. 1988;48:3221–3229.
20. Carney DN, Marangos PJ, Ihde DC, et al. Serum neuron-specific enolase: a marker for disease extent and response to therapy of small-cell lung cancer. *Lancet*. 1982;1:583–585.
21. Burghuber OC, Worofka B, Scherthaner G, et al. Serum neuron-specific enolase is a useful tumor marker for small cell lung cancer. *Cancer*. 1990;65:1386–1390.
22. Muraki M, Tohda Y, Iwanaga T, Uejima H, Nagasaka Y, Nakajima S. Assessment of serum CYFRA 21-1 in lung cancer. *Cancer*. 1996;77:1274–1277.
23. Keller T, Bitterlich N, Hilfenhaus S, Bigl H, Loser T, Leonhardt P. Tumor markers in the diagnosis of bronchial carcinoma: new options using fuzzy logic-based tumor marker profiles. *J Cancer Res Clin Oncol*. 1998;124:565–574.
24. Martin WH, Delbeke D, Patton JA, Sandler MP. Detection of malignancies with SPECT versus PET with 2-[fluorine-18]fluoro-2-deoxy-D-glucose. *Radiology*. 1996;198:225–231.
25. Brown RS, Leung JY, Kison PV, Zasadny KR, Flint A, Wahl RL. Glucose transporters and FDG uptake in untreated primary human non-small cell lung cancer. *J Nucl Med*. 1999;40:556–565.
26. Delbeke D, Patton JA, Martin WH, Sandler MP. FDG PET and dual-head gamma camera positron coincidence detection imaging of suspected malignancies and brain disorders. *J Nucl Med*. 1999;40:110–117.
27. Tatsumi M, Yutani K, Watanabe Y, et al. Feasibility of fluorodeoxyglucose dual-head gamma camera coincidence imaging in the evaluation of lung cancer: comparison with FDG PET. *J Nucl Med*. 1999;40:566–573.
28. Weber W, Young C, Abdel-Dayem M, et al. Assessment of pulmonary lesions with ¹⁸F-fluorodeoxyglucose positron imaging using coincidence mode gamma cameras. *J Nucl Med*. 1999;40:574–578.
29. Strauss LG. Fluorine-18 deoxyglucose and false-positive results: a major problem in the diagnostics of oncological patients. *Eur J Nucl Med*. 1996;23:1409–1415.
30. Lowe VJ, Duhaylongsod FG, Patz EF, et al. Pulmonary abnormalities and PET data analysis: a retrospective study. *Radiology*. 1997;202:435–439.
31. Kapucu LO, Meltzer CC, Townsend DW, Keenan RJ, Luketich JD. Fluorine-18-fluorodeoxyglucose uptake in pneumonia. *J Nucl Med*. 1998;39:1267–1269.
32. Degirmenci B, Zeftawy HA, Atay S, et al. F-18 FDG dual head gamma camera coincidence imaging in evaluation of tumor/background ratio in pulmonary lesions [abstract]. *Turk J Nucl Med*. 1998;7:35.
33. Jang HJ, Lee KS, Kwon OJ, Rhee CH, Shim YM, Han J. Bronchioloalveolar carcinoma: focal area of ground-glass attenuation at thin-section CT as an early sign. *Radiology*. 1996;199:485–488.
34. Higashi K, Ueda Y, Seki H, et al. Fluorine-18-FDG PET imaging is negative in bronchioloalveolar carcinoma. *J Nucl Med*. 1998;39:1016–1020.
35. Imran MB, Kubota K, Yamada S, et al. Lesion-to-background ratio in nonattenuation-corrected whole-body FDG PET images. *J Nucl Med*. 1998;39:1219–1223.
36. Fukuda I, Yamakado M, Kiyose H. Influence of smoking on serum carcinoembryonic antigen levels in subjects who underwent multiphasic health testing and services. *J Med Syst*. 1998;22:89–93.
37. Stockley RA, Shaw J, Whitfield AG, Whitehead TP, Clarke CA, Burnett D. Effect of cigarette smoking, pulmonary inflammation, and lung disease on concentrations of carcinoembryonic antigen in serum and secretions. *Thorax*. 1986;41:17–24.
38. Alexander JC, Silverman NA, Chretien PB. Effect of age and cigarette smoking on carcinoembryonic antigen levels. *JAMA*. 1976;235:1975–1979.
39. Scott WJ, Shepherd J, Gambhir SS. Cost-effectiveness of FDG-PET for staging non-small cell lung cancer: a decision analysis. *Ann Thorac Surg*. 1998;66:1876–1883.